Thresholdless microlaser

F. De Martini, F. Cairo, P. Mataloni, and F. Verzegnassi
Dipartimento di Fisica dell'Università "La Sapienza," Roma, 00185 Italy
(Received 3 March 1992)

The near-zero threshold and the very high gain of the active optical microlaser are investigated both theoretically and experimentally. These properties are found to be determined by the synergy of several quantum-statistical processes taking place in the condition of *extreme* field confinement provided by the peculiar Casimir-type topology of the optical microcavity. The determination of the microcavity mode structure leads to a detailed study of the process of merging of the spontaneous emission with stimulated emission (StE) and of the consequent anomalous onset of the collective atomic behavior at very low excitation levels. An excitation threshold of about 50 pJ has been determined experimentally with a molecular oxazine microlaser excited by a femtosecond-pulse source. The relevance within the overall StE dynamics of the processes of mode-competition fluorescence loss, interatom transverse Bose correlations, and periodic excitation are investigated both theoretically and experimentally. A discussion of the overall process in terms of a second-order phase transition in a nonequilibrium statistical problem is given. The extension of the microcavity dynamics to quantum-dynamical systems such as the "microscopic" parametric oscillator and to Raman and Compton scattering is also considered.

PACS number(s): 42.50.Fx, 03.65.−w, 12.20.Fv

I. INTRODUCTION

High gain and a near-zero-threshold have been recognized to be distinctive properties of the microscopic laser (microlaser) since its original proposal and realization [1]. This peculiar phenomenology, of obvious interest for modern technology, is in fact rooted in the fundamental quantum dynamics of the collective atom-radiation coupling process. What looks interesting in this respect is that the overall striking behavior of the device results from a synergy of several different physical processes that are independently affected in a favorable manner by the microlaser geometry. First, the spontaneous emission (SpE) of a *single atom* is strongly affected by the *extreme* vacuum confinement determined by the Casimir-type one-dimensional topology of the Fabry-Pérot (FP) microscopic cavity (microcavity) [2–4]. There in fact microcavity spacings $d = n\bar{d}$, $\bar{d} \equiv (\lambda/2)$ with n a whole number (WN) determine the "enhancement" of the coupling strength of a single atom with the field, a well-known manifestation of the increasing field density of states for decreasing d. Second, the decrease of d implies at the same time a decrease of the number n of longitudinal cavity modes available for atomic deexcitation [1,4]. If N is the number of excited atoms present in the cavity, a decrease of d implies that an increasingly larger number of atoms $N_n \equiv (N/n)$ will eventually cooperate by the stimulated emission (StE) taking place on each mode. This in turn leads to a most important anomalous quantum-dynamical condition, i.e., for large N_n the "vacuum state" is practically nonexistent as it is "occupied" very quickly by the first SpE photon emitted by an atom within the coherence time. Then the Bose-Einstein inter-atom correlations determine a collective behavior with a sudden onset of stimulated emission with exponential gain. From the perspective of statistical mechanics, this anomalous merging of SpE into StE may be understood as a consequence of the lowering of the relevant dissipation process provided by fluorescence loss and mode competition. This is partially due to a reduction of the dimensionality of the mode-statistical ensemble toward a single degree-of-freedom condition which implies the elimination of the statistical-mode "reservoir" and a quick establishment of a "collective" state in the medium. By reversing the argument, the usual macroscopic laser condition is reached by increasing $d > \bar{d}$, i.e., when additional modes become available for atomic deexcitation. There the original orderly system at $d = \bar{d}$ becomes a "chaotic" system with rapidly increasing complexity. This leads to the appearance of mode competition and fluorescence loss with reduction of gain and increase of the threshold pumping level. The dynamics of the complex laser system is generally investigated by the methods of nonequilibrium statistical mechanics, i.e., by the Fokker-Planck method [5] and by the second-order phase-transition theory [6]. In the context of the latter theory the behavior of the microlaser may be understood by analogy with the phenomenologies of ferromagnetism and superconductivity. In our cooperative system the "order" process is overwhelming the "disorder" provided by cavity losses so much that once one photon is stored in the cavity, any additional emission process provides the symmetry-breaking field to establish a phase transition to the state on nonzero average field $\langle E \rangle$, i.e., to the Glauber's state $|\alpha\rangle$. In nonequilibrium laser phase-transition theory the resulting virtual cancellation in the disorder phase leads to a zero value of the critical "reservoir variable," which is the threshold population inversion" $\sigma_t = N_t \approx 0$. Then by analogy with equilibrium problems, the microlaser may be thought of as behaving as an extremely high-critical-temperature (T_c) ferromagnet or superconductor [6]. In the present work we do not pursue any further the phase-transition analogy as the "single-degree-of-freedom" condition results quite natu-

rally from the QED analysis of the interaction of the atoms with one or few cavity modes. The work is organized as follows. In Sec. II the structure of the modes is investigated following closely the corresponding theory given in Ref. [3]. This leads to the field quantization in Sec. III and to the derivation in Sec. IV of the emission rates for SpE and StE in a *collective* (i.e., multiatom) regime. There the effect of different excitation distributions is investigated. A steady-state single-mode laser theory is given in Sec. V showing the dynamical origin of the thresholdless and high-gain behavior of the microlaser. These findings are substantiated by the experimental results reported in Sec. VI, while in Sec. VII the interplay of the thresholdless dynamics with the "laser phase-matching" process is shown. The application of the same process to SpE allows a direct determination of the field energy distribution in an optical cavity.

II. TRAVELING-WAVE MODES OF A FABRY-PÉROT CAVITY

In order to calculate the atomic emission rates in a Fabry-Pérot cavity we first determine the appropriate spatial modes for quantization of the electromagnetic field [3]. Refer to Fig. 1: The z axis is taken normal to the mirrors with its origin in the middle of the cavity. The mirrors are assumed to have infinite extents in the xy plane. As it is represented in the Fig. 1, multiple reflections couple together waves of wave vectors

$$\begin{aligned}\mathbf{k}_+ &= k(\sin\Theta\cos\Phi\ ,\sin\Theta\sin\Phi\ ,\cos\Theta)\ ,\\ \mathbf{k}_- &= k(\sin\Theta\cos\Phi\ ,\sin\Theta\sin\Phi\ ,-\cos\Theta)\end{aligned} \tag{2.1}$$

for $(0\le\Theta\le\frac{1}{2}\pi)$. Four distinct spatial modes can be constructed from contributions with the same two wave vectors. For each set of polar angles Θ and Φ, there are two transverse polarization directions whose unit vectors are chosen to be

$$\epsilon(\mathbf{k}_+,1)=\epsilon(\mathbf{k}_-,1)=(\sin\Phi\ ,-\cos\Phi\ ,0)\ , \tag{2.2}$$

$$\begin{aligned}\epsilon(\mathbf{k}_+,2)&=(\cos\Theta\cos\Phi\ ,\cos\Theta\sin\Phi\ ,-\sin\Theta)\ ,\\ \epsilon(\mathbf{k}_-,2)&=(\cos\Theta\cos\Phi\ ,\cos\Theta\sin\Phi\ ,\sin\Theta)\ ,\end{aligned} \tag{2.3}$$

where the $\mathbf{k}_+$ and $\mathbf{k}_-$ designations indicate the polarizations of the respective wave-vector contributions. It is convenient to indicate the polarizations in (2.2) and (2.3) by an index $j=1,2$. The complex reflection and transmission coefficients r_{1j},t_{1j} and r_{2j},t_{2j} of the cavity mirrors are generally different for the two polarizations and depend on the polar angle Θ [7]. They are assumed to have the following unitary lossless properties for all values of Θ:

$$|r_{1j}|^2+|t_{1j}|^2=|r_{2j}|^2+|t_{2j}|^2=1\ , \tag{2.4}$$

$$r_{1j}^*t_{1j}+r_{1j}t_{1j}^*=r_{2j}^*t_{2j}+r_{2j}t_{2j}^*=0\ , \tag{2.5}$$

where r_{ij}^*,t_{ij}^* are complex conjugates (c.c.'s) of r_{ij},t_{ij}. Optical propagation within the mirrors is not important for the present study, and we accordingly ignore their internal mode structure. For each pair of coupled wave vectors $\mathbf{k}_+$, $\mathbf{k}_-$ designated by $\mathbf{k}$ for brevity, and for each transverse polarization there are two distinct mode functions corresponding to incoming plane waves of unit amplitude that are incident, respectively, from the negative and positive z sides of the cavity. The forms of these functions are obtained, as usual in Fabry-Pérot theory, by summing the geometric series resulting from the multiple reflections in the mirrors [7,8]. The two kinds of spatial dependence are thus given as follows:

Mode function $U_{\mathbf{k}j}(\mathbf{r})$

$\exp(i\mathbf{k}_+\cdot\mathbf{r})$	$R_{\mathbf{k}j}\exp(i\mathbf{k}_-\cdot\mathbf{r})$	$-\infty<Z<-\frac{1}{2}d$
$t_{1j}\exp(i\mathbf{k}_+\cdot\mathbf{r})/D_j$	$t_{1j}r_{2j}\exp(i\mathbf{k}_-\cdot\mathbf{r}+ikd\cos\Theta)/D_j$	$-\frac{1}{2}d<Z<+\frac{1}{2}d$
$T_{\mathbf{k}j}\exp(i\mathbf{k}_+\cdot\mathbf{r})$	0	$+\frac{1}{2}d<Z<+\infty$

(2.6)

Mode function $U'_{\mathbf{k}j}(\mathbf{r})$

$T'_{\mathbf{k}j}\exp(i\mathbf{k}_-\cdot\mathbf{r})$	0	$-\infty<Z<-\frac{1}{2}d$
$t_{2j}\exp(i\mathbf{k}_-\cdot\mathbf{r})/D_j$	$t_{2j}r_{1j}\exp(i\mathbf{k}_+\cdot\mathbf{r}+ikd\cos\Theta)/D_j$	$-\frac{1}{2}d<Z<+\frac{1}{2}d$
$\exp(i\mathbf{k}_-\cdot\mathbf{r})$	$R'_{\mathbf{k}j}\exp(i\mathbf{k}_+\cdot\mathbf{r})$	$+\frac{1}{2}d<Z<+\infty$

(2.7)

where the expressions in each row of (2.6) and (2.7) represent, as shown in Fig. 1, the plane-wave mode functions propagating in the space portions indicated at the rhs and excited for the sets $U_{\mathbf{k}j}$ and $U'_{\mathbf{k}j}$ by the waves $\exp(i\mathbf{k}_+\cdot\mathbf{r})$ and $\exp(i\mathbf{k}_-\cdot\mathbf{r})$, respectively. In (2.6) and (2.7) the various quantities are defined as

$$D_j\equiv[1-r_{1j}r_{2j}\exp(2ikd\cos\Theta)]\ , \tag{2.8}$$

$$\begin{aligned}R_{\mathbf{k}j}\equiv[&r_{1j}\exp(-ikd\cos\Theta)\\ &+r_{2j}(t_{1j}^2-r_{1j}^2)\exp(ikd\cos\Theta)]/D_j\ ,\end{aligned} \tag{2.9}$$

$$T_{\mathbf{k}j}\equiv T'_{\mathbf{k}j}=t_{1j}t_{2j}/D_j\ , \tag{2.10}$$

$$\begin{aligned}R'_{\mathbf{k}j}\equiv[&r_{2j}\exp(-ikd\cos\Theta)\\ &+r_{1j}(t_{2j}^2-r_{2j}^2)\exp(ikd\cos\Theta)]/D_j\ .\end{aligned} \tag{2.11}$$

The last three quantities represent the reflection and transmission coefficients of the cavity as a whole. With the use of (2.4) and (2.5) they satisfy

$$|R_{\mathbf{k}j}|=|R'_{\mathbf{k}j}|\ , \tag{2.12}$$

$$|R_{\mathbf{k}j}|^2+|T_{\mathbf{k}j}|^2=|R'_{\mathbf{k}j}|^2+|T'_{\mathbf{k}j}|^2=1\ , \tag{2.13}$$

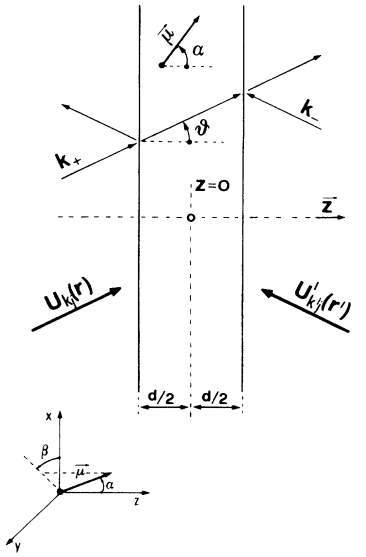

FIG. 1. Geometry of the Fabry-Pérot microcavity showing the two kinds of modes and the geometrical orientation of the emitting dipole μ. Mirrors labeled by 1,2 in the text are represented, respectively, at the left and right of the figure.

$$R^*_{\mathbf{k}j}T'_{\mathbf{k}j}+R'_{\mathbf{k}j}T^*_{\mathbf{k}j}=0\ . \tag{2.14}$$

These properties ensure the normalization and orthogonality of the two modes that have the same wave vectors and polarizations, and the general relations are

$$\int d\mathbf{r}\,\boldsymbol{\epsilon}(\mathbf{k},j)\cdot\boldsymbol{\epsilon}(\mathbf{k}',j')U_{\mathbf{k}j}(\mathbf{r})U'^*_{\mathbf{k}'j'}(\mathbf{r})=0\ , \tag{2.15}$$

$$\int dr\,\boldsymbol{\epsilon}(\mathbf{k},j)\cdot\boldsymbol{\epsilon}(\mathbf{k}'j')U_{\mathbf{k}j}(\mathbf{r})U^*_{\mathbf{k}'j'}(\mathbf{r}) =(2\pi)^3\delta_{ij'}\delta(\mathbf{k}-\mathbf{k}') \tag{2.16}$$

together with the identical normalization integral for the primed mode function (2.7). The modes (2.6) and (2.7) form a complete set of functions for all of space, including the interior of the cavity and the exterior regions on either side. They allow calculations to be made of the SpE and StE rates and radiated-field operators for atoms that are excited in cavities whose mirrors both transmit nonzero fractions of the emitted intensity. In the limiting case of a perfectly reflecting closed cavity, the traveling-wave mode functions used here reproduce results ordinarily obtained with standing-wave modes, while in the opposite extreme of an absent cavity, the mode functions (2.6) and (2.7) taken together produce the usual complete set of plane waves in infinite free space. In intermediate conditions the modes form a convenient basis for general calculations, and they are free of the potential limitations inherent in modes restricted to exterior regions of finite extent or to only one side of the cavity. Several mathematical expressions encountered in the present and in further sections can be simplified in cases of physical relevance for the problem at hand. A typical simplification relates to the *high-Q* and *symmetric* cavity for which $r_{1j}=r_{2j}=r_j=-|r_j|$ and $t_{1j}=t_{2j}=t_j=i|t_j|$. In this case and for the purpose of easing the integrations involved in the evaluation of the cross section considered later, also the expression of the resonant Airy function $|D_j|^{-2}$ can be simplified substantially. In fact, owing to (2.8), the Airy function Y can be written as

$$\begin{aligned}Y=1/|D_j|^2&\equiv[(1-|r_j|^2)^2+4|r_j|^2\sin w]^{-1}\\&\approx\sum_{l=0}^{\infty}\{[2|r_j|(w-l\pi)]^2+[1-|r_j|^2]^2\}^{-1}\end{aligned} \tag{2.17}$$

$$\begin{aligned}&\approx\{\pi/[2k_0d|r_j|(1-|r_j|^2)]\}\\&\quad\times\left[\tfrac{1}{2}\delta(C)+\sum_{l=1}^{n}\delta(C-(l\pi/k_0d))\right]\\&=[2n|r_j|(1-|r_j|^2)]^{-1}\\&\quad\times\left[\tfrac{1}{2}\delta(C)+\sum_{l=1}^{n}\delta(C-1/n)\right],\\&\qquad C\equiv\cos\Theta\ ,\ n\equiv k_0d/\pi=d/\bar{d}\ .\end{aligned} \tag{2.18}$$

Equation (2.18) is written in terms of the two nonnegative parameters n and l. Both parameters are taken thereafter as whole numbers and represent the microcavity order $n\equiv(2d/\lambda)\geq 1$ and the mode order $0<l\leq n$, respectively [2]. In particular, note that this assumption taken for n expresses, within the stated approximations, a cavity dimension d corresponding to the well-known condition of enhancement of all atom-field interaction processes, including spontaneous and stimulated emission [1,2,3,9]. In the present work only that dynamical condition and the related values of n and d are taken into consideration. The expressions (2.17) and (2.18) are valid for a microcavity having a large FP finesse f [7]

$$f=[\pi|r|/(1-|r|^2)]\gg 1\ . \tag{2.19}$$

III. FIELD QUANTIZATION

The electromagnetic field is quantized by the introduction of mode creation and destruction operators. The operators for the modes with spatial functions $U_{\mathbf{k}j}(\mathbf{r})$ and $U'_{\mathbf{k}j}(\mathbf{r})$ are denoted $\hat{a}^\dagger_{\mathbf{k}j}$, $\hat{a}_{\mathbf{k}j}$ and $\hat{a}'^\dagger_{\mathbf{k}j}$, $\hat{a}'_{\mathbf{k}j}$, respectively, where $j=1,2$ indicates the choice of mode polarization (2.2) or (2.3). With $\mathbf{k}$ taken to be a continuous variable, the operators satisfy the commutation relations,

$$\begin{aligned}&[\hat{a}_{\mathbf{k}j},\hat{a}^\dagger_{\mathbf{k}'j'}]=[\hat{a}'_{\mathbf{k}j},\hat{a}'^\dagger_{\mathbf{k}'j'}]=\delta_{jj'}\delta(\mathbf{k}-\mathbf{k}')\ ,\\&[\hat{a}_{\mathbf{k}j},\hat{a}'^\dagger_{\mathbf{k}'j'}]=\hat{a}'_{\mathbf{k}j},\hat{a}^\dagger_{\mathbf{k}'j'}]=0\ .\end{aligned} \tag{3.1}$$

The electromagnetic field quantization now proceeds in the usual way, and we need quote only the main results [9]. The Heisenberg electric-field operator is conveniently separated into two parts

$$\hat{\mathbf{E}}(\mathbf{r},t)=\hat{\mathbf{E}}^+(\mathbf{r},t)+\hat{E}^-(\mathbf{r},t)\ , \tag{3.2}$$

where

$$\hat{\mathbf{E}}^{+}(\mathbf{r},t)=i\int d\mathbf{k}\sum_{j}(\hbar kc/16\pi^3\epsilon_0)^{1/2}\epsilon(\mathbf{k},j)\times[U_{\mathbf{k}j}(r)\hat{a}_{\mathbf{k}j}+U'_{\mathbf{k}j}(r)\hat{a}'_{\mathbf{k}j}]\times\exp(-ickt) \tag{3.3}$$

and $\hat{\mathbf{E}}^{-}(\mathbf{r},t)$ is given by the Hermitian conjugate (H.c.) expressions. In writing out the field operators explicitly, the polarization vectors, given by (2.2) and (2.3), are those associated with the wave vectors k_- or k_+ appropriate to the corresponding terms in the mode functions, given by (2.6) and (2.7). Because of the way in which wave-vector space is divided into two half spaces by the cavity, the three-dimensional integral in (3.3) is

$$\int dk=\int_0^{\infty}dk\int_0^{1/2\pi}d\Theta\int_0^{2\pi}d\Phi\,k^2\sin\Theta\ . \tag{3.4}$$

The normal-ordered part of the free-field Hamiltonian is

$$\hat{H}^0=\int d\mathbf{k}\,\hbar ck\sum_j(\hat{a}^{\dagger}_{\mathbf{k}j}\hat{a}_{\mathbf{k}j}+\hat{a}'^{\dagger}_{\mathbf{k}j}\hat{a}'_{\mathbf{k}j})\ ,\quad j=1,2\ , \tag{3.5}$$

and the Hamiltonian for interaction of the field with an atomic electric-dipole transition of matrix element $\boldsymbol{\mu}$ located at position $\mathbf{r}_0$ inside the cavity is $\hat{H}^I=\sum_k\hat{H}^I_k$. $\hat{H}^I_k$ is the contribution due to the interaction of the dipole with any single-cavity $\mathbf{k}$ mode. In that case only the expressions of the quantum fields defined in that mode are to be taken into consideration

$$\hat{H}^I_k=i\int_k d\mathbf{k}\sum_j(\hbar ck/16\pi^3\epsilon_0)^{1/2}\exp(-ickt)/D_j\times\{\hat{a}_{\mathbf{k}j}[\epsilon(\mathbf{k}_+,j)t_{1j}\exp(i\mathbf{k}_+\cdot\mathbf{r}_0)+\epsilon(\mathbf{k}_-,j)t_{1j}r_{2j}\exp(i\mathbf{k}_-\cdot\mathbf{r}_0+ikd\cos\Theta)]+\hat{a}'_{\mathbf{k}j}[\epsilon(k_-,j)t_{2j}\exp(i\mathbf{k}_-\cdot\mathbf{r}_0)+\epsilon(\mathbf{k}_+,j)t_{2j}r_{1j}\exp(i\mathbf{k}_+\cdot\mathbf{r}_0+ikd\cos\Theta)]\}\cdot\boldsymbol{\mu}+\text{ H.c.}\ , \tag{3.6}$$

where (2.6) and (2.7) have been used and the integration is carried out over the angular extent of the cavity $\mathbf{k}$ mode.

IV. EMISSION RATES: SPONTANEOUS EMISSION

The spontaneous emission (SpE) rate is calculated for the decay of an atom in the vacuum field of the cavity from an excited state of energy $\hbar ck_0$ to the atomic ground state. Assume that Markov approximation holds, and the SpE rate can be obtained by the application of Fermi's golden rule. We use the commutation properties (3.1) with the total interaction Hamiltonian $\hat{H}^I$ and the result

$$(\mathbf{k}_+-\mathbf{k}_-)\cdot\mathbf{r}_0=2kz\cos\Theta \tag{4.1}$$

z being the relevant coordinate of the atom. The SpE rate for an atomic assembly belonging to a layer parallel to mirrors, with coordinate z and thickness dz, is

$$\Gamma(z)=\int d\mathbf{k}\sum_j(k/8\pi^2\epsilon_0\hbar)(|\{\epsilon(\mathbf{k}_+,j)t_{1j}+\epsilon(\mathbf{k}_-,j)t_{1j}r_{2j}\exp[ik(d-2z)\cos\Theta]\}\cdot\boldsymbol{\mu}|^2+|\{\epsilon(\mathbf{k}_-,j)t_{2j}+\epsilon(\mathbf{k}_+,j)t_{2j}r_{1j}\exp[ik(d+2z)\cos\Theta]\}\cdot\boldsymbol{\mu}|^2)\delta(k-k_0)/|D_j|^2\ . \tag{4.2}$$

It is convenient to calculate separately the contributions to the SpE rate from the components of the transition dipole moment $\boldsymbol{\mu}$ parallel and perpendicular to the cavity mirrors. For the parallel contribution, we assume with no loss of generality that $\boldsymbol{\mu}$ is parallel to the x axis, so that (2.2) and (2.3) give

$$\begin{aligned}&\epsilon(\mathbf{k}_+,1)\cdot\boldsymbol{\mu}=\epsilon(\mathbf{k}_-,1)\cdot\boldsymbol{\mu}=\mu\sin\Phi\ ,\\&\epsilon(\mathbf{k}_+,2)\cdot\boldsymbol{\mu}=\epsilon(\mathbf{k}_-,2)\cdot\boldsymbol{\mu}=\mu\cos\Theta\cos\Phi\ .\end{aligned} \tag{4.3}$$

The k and Φ integrations, as defined in (3.4), can now be performed, and with the Θ integral simplified by a change of variable to $C\equiv\cos\Theta$, the emission rate is

$$\Gamma_{\parallel}(z)=(3\Gamma_0/8)\int_0^1 dC\{[(1-|r_{11}|^2)|1+r_{21}\exp(2iw_-)|^2+(1-|r_{21}|^2)|1+r_{11}\exp(2iw_+)|^2]|D_1|^{-2}+[(1-|r_{12}|^2)|1+r_{22}\exp(2iw_-)|^2+(1-|r_{22}|^2)|1+r_{12}\exp(2iw_+)|^2]|C/D_2|^2\}\ , \tag{4.4}$$

where

$$\Gamma_0\equiv k_0^3\mu^2/(3\pi\epsilon_0\hbar)\equiv(T_0)^{-1} \tag{4.5}$$

is the usual free-space SpE rate [9], k is replaced by k_0 in the expression (2.8) for D_j, (2.4) has been used to express the emission rate entirely in terms of the Θ-dependent mirror reflectivities, and

$$\begin{aligned}&w_+\equiv k_0(\tfrac{1}{2}d+z)C\ ,\quad w_-\equiv k_0(\tfrac{1}{2}d-z)C\ ,\\&w\equiv k_0dC\ ,\quad C\equiv\cos\Theta\ .\end{aligned} \tag{4.6}$$

The SpE rate for a $\boldsymbol{\mu}$ perpendicular to the mirrors or parallel to the z axis is calculated in a similar fashion. The polar-

izations (2.2) and (2.3) now give,

$$\epsilon(\mathbf{k}_+,1)\cdot\boldsymbol{\mu}=\epsilon(\mathbf{k}_-,1)\cdot\boldsymbol{\mu}=0\ ,$$
$$\epsilon(\mathbf{k}_+,2)\cdot\boldsymbol{\mu}=-\epsilon(\mathbf{k}_-,2)\cdot\boldsymbol{\mu}=-\mu\sin\Theta \tag{4.7}$$

and the emission rate (4.2) becomes,

$$\Gamma_\perp(z)=(3\Gamma_0/4)\int_0^1 dC(1-C^2)|1-r_{12}r_{22}\exp(2iw)|^{-2}$$
$$\times[(1-|r_{12}|^2)|1-r_{22}\exp(2iw_-)|^2+(1-|r_{22}|^2)|1-r_{12}\exp(2iw_+)|^2] \tag{4.8}$$

after partial integration as before. The above expressions simplify in various special cases, as shown in Ref. [3]. the condition of symmetrical cavity expressed by

$$r_{1j}=r_{2j}=r_j=-|r_j| \quad \text{and} \quad t_{1j}=t_{2j}=t_j=i|t_j| \tag{4.9}$$

should be worked out in some detail as it represents our experimental condition. By the use of (4.9) the integrands in (4.4) and (4.8) can be put in forms more convenient for computation, as

$$\Gamma_\parallel(z)=(3\Gamma_0/4)\int_0^1 dC[F_1(C)+C^2F_2(C)] \tag{4.10}$$

and

$$\Gamma_\perp(z)=(3\Gamma_0/2)\int_0^1 dC(1-C^2)G_2(C) \tag{4.11}$$

where

$$F_1(C)\equiv[(1-|r_1|)^2+2|r_1|(\sin^2w_-+\sin^2w_+)]/[1-|r_1|^2+4(|r_1|^{-2}-1)^{-1}\sin^2w]\ ,$$
$$G_2(C)\equiv[(1-|r_2|)^2+2|r_2|(\cos^2w_-+\cos^2w_+)]/[1-|r_2|^2+4(|r_2|^{-2}-1)^{-1}\sin^2w]\ .$$

$F_2(C)$ is obtained by substituting r_1 by r_2 in the expression of $F_1(C)$. Figure 2 shows the SpE rates for a dipole in the condition of extreme confinement $d=\bar{d}$. These expressions can be combined to give the SpE rate for a transition whose dipole moment has an isotropic spatial distribution as

$$\Gamma(z)=[2\Gamma_\parallel(z)+\Gamma_\perp(z)]/3$$
$$=\tfrac{1}{2}\Gamma_0\int_0^1 dC(F_1(C)+[1-|r_2|^2+4(|r_2|^{-2}-1)^{-1}\sin^2w]^{-1}$$
$$\times\{(1+|r_2|)^2-2|r_2|[\sin^2w_-+\sin^2w_++2C^2\cos w\cos(2k_0Cz)]\})\ . \tag{4.12}$$

The above integrals can be calculated easily by making the additional approximation of high-Q cavity i.e., by considering the limit $|r_j|\to 1$, $|t_j|\to 0$, $f\to\infty$, and the results (2.18). For a single atom, the rate of spontaneous emission over *all* modes of a very high-Q cavity, with order $n=kd/\pi$, is now found to be

$$\Gamma_n(z)=\Gamma_0\left[\tfrac{1}{2}+n-\sum_{l=1}^{n}(-1)^l(l/n)^2\cos(2\pi lz/d)\right]\Big/n\ . \tag{4.13}$$

By this expression we may also calculate for a single atom the rate $\Gamma_{l,n}$ of spontaneous emission over any particular cavity mode order $l\le n$ and for one polarization by assuming, by a further approximation, that $|r_j|$ and $|t_j|$ do not depend on the polarization of the fields

$$\Gamma_{l,n}(z)=\tfrac{1}{2}\Gamma_0[(n^2-l^2)+2l^2f^2(x)]/n^3\ ,\quad x\equiv(z/d) \tag{4.14}$$

where

$$f^2(x)\equiv\cos^2(\pi lx) \text{ for } l=\text{an odd whole number}\ ,$$
$$f^2(x)\equiv\sin^2(\pi lx) \text{ for } l=\text{an even WN}\ . \tag{4.15}$$

Let us consider now an ensemble of excited atoms in the cavity and suppose that no superradiant effects are present [2,3]. The corresponding SpE rates Γ_n and $\Gamma_{l,n}$ are obtained by averaging $\Gamma_n(z)$ over the normalized distribution density $g(z)$ of excited atoms in the cavity. Various kinds of excitation distributions may be considered. For instance, the atoms may fill out the cavity with uniform density and $g(z)=d^{-1}$. In this case the contribution of the sum of cos functions in (4.13) is zero and the rates are $\Gamma_n=\frac{1}{2}\Gamma_0(1+2n)/n$ and $\Gamma_{l,n}=\frac{1}{2}\Gamma_0/n$ (l independent).

Alternatively, $g(z)$ may be expressed by a sum of n' δ functions whose arguments may be chosen to enhance the contributions of the l modes in (4.13) and (4.14). For instance we may take $n'=n$ δ functions peaked at coordinates equally spaced over the cavity spacing $g(|z|)=(1/n')\sum_{l'}\delta[|z-(dl'/2n)|]$, where l' is an even whole number $0\le l'<n$, if n is odd and vice versa. The

simplest configuration, appropriate for odd cavity order n, is represented by $g(z)=\delta(z)$, i.e., by a single excitation δ function placed at the center of the cavity. This condition may be approximated by a semiconductor microlaser operating with a thin active quantum well placed at $z=0$ [10]. In this case the emission rates are $\Gamma_n=\Gamma_0[(1+n)+(2n)^{-1}]/n$, and $\Gamma_{l,n}=\frac{1}{2}\Gamma_0(n^2+l^2)/n^3$ for odd l, $\Gamma_{l,n}=\frac{1}{2}\Gamma_0(n^2-l^2)/n^3$ for even l. Another interesting configuration, adopted in one experiment described later, leads to a substantial enhancement of Γ_n and of $\Gamma_{l,n}$. It corresponds to an excitation distribution $g(z)$ provided by a single (or a combination of) sinusoidal function of z with periodicity expressed by an excitation wave vector $\bar{k}$. In this way it is possible to enhance selectively the rates of SpE taking place over any of the $\mathbf{k}_l$ modes, the ones corresponding to the lth cavity order. We refer to this process as a laser-phase-matching (LPM) process, which is expressed, in the simple case of $g(z)$ given by a single sinusoidal function, by the resonant condition in the momentum k space:

$$\Delta\mathbf{k}\equiv(\mathbf{k}-\mathbf{k}_l)=\mathbf{0} \quad \text{(laser phase matching)} , \tag{4.16}$$

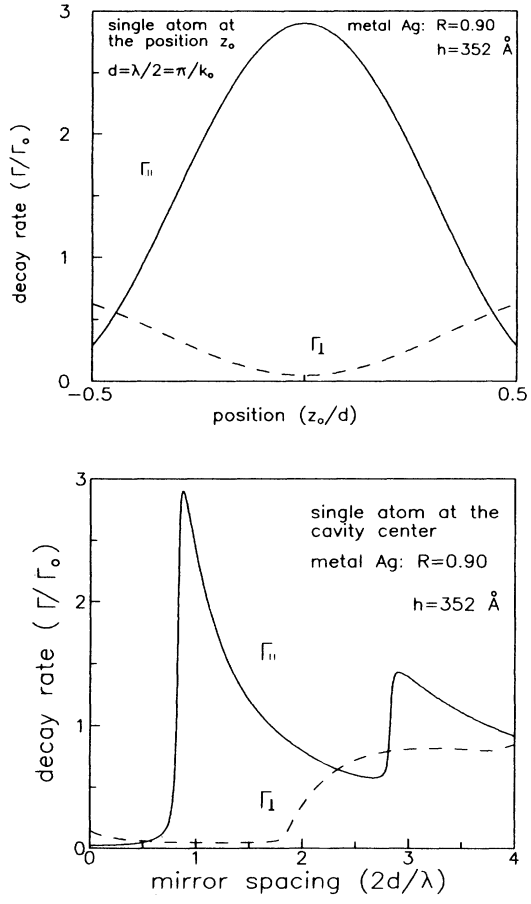

FIG. 2. Decay rate $\Gamma_{\parallel}(z)$ and $\Gamma_{\perp}(z)$ of a single dipole μ placed at position z with orientation, respectively, parallel and orthogonal to the mirrors in a symmetrical microcavity confined by Ag mirrors with normal reflectivity $R=0.90$ at $\lambda=6111$ Å (upper panel). Decay rates of a dipole placed at the center $z=0$ of a symmetrical microcavity as a function of the cavity spacing (lower panel).

where $|\mathbf{k}_l|=l(\pi/d)$ [11]. Most important for our present work, we shall see in a later section that the same process shows up also in stimulated emission thus providing a substantial enhancement of the microlaser gain. The LPM process in SpE and StE will be demonstrated experimentally later for a microcavity with $n=1$ making recourse to the technique of periodic excitation [12]. The simplest normalized distribution for StE enhancement over the l' mode can be expressed by

$$g(x)=(2/d)\cos^2(\pi l' x) . \tag{4.17}$$

Making use of (4.17), we may calculate the SpE rates corresponding to LPM emission over the lth mode for a cavity-order $n=$odd number [13]. These are

$$\Gamma_n=\Gamma_0[(n+1)+(2n)^{-1}-(-1)^{l'}(l'/n)^2]/n$$

$$\Gamma_{l,n}=\tfrac{1}{2}\Gamma_0(n^2+\tfrac{1}{2}l^2)/n^3 \quad \text{for} \quad l'=l ,$$

$$\Gamma_{l,n}=\tfrac{1}{2}\Gamma_0/n \quad \text{for} \quad l'\neq l .$$

No enhancement is provided for emission over the $\mathbf{k}_l$ mode if $l'\neq l$. Similar conclusions can be drawn for any cavity order expressed by even n number by replacing in (4.17) the $\cos^2(\pi l' x)$ function with $\sin^2(\pi l' x)$. In fact inspection of (4.14) shows that, in general, the rates of spontaneous or stimulated emission over a particular microcavity mode $\mathbf{k}_l$ with *any* order $l\leq n$ can be increased (or decreased) by selecting a distribution of atomic excitation that is periodic along the z axis with periodicity $(\pi l/d)$ and appropriate phase. The reader should be warned, once again, about a relevant approximation which is implied by the above calculations. In fact the expressions above have been evaluated by assuming for the sake of simplicity, that the mirror coatings are infinitely thin and that the reflectivities are independent of Θ and that fields undergo a Θ-independent phase change $\phi=\pi$ upon reflection. We recall that the Θ dependence of field reflectivities, transmitivities, and phases realized in actual cases with any kind of mirror coating may lead to quite different results for $\Gamma_{\parallel}(z_0)$ and $\Gamma_{\perp}(z_0)$ [3,7].

V. STIMULATED EMISSION

The rate of stimulated emission (StE) over a single-cavity $\mathbf{k}$ mode is found by a similar method by adopting in the Fermi rule the expression of the corresponding partial Hamiltonian H_k^I given by (3.6). This approximation, which is valid for low excitation and near-threshold operation, implies absence of coupling between different cavity modes. In this way the dynamical equation accounting for laser action can be obtained easily. We shall later demonstrate that this equation leads to a most favorable behavior of the microlaser. Precisely, as previously discussed, a very high microlaser gain can be attained and the threshold-pumping energy can reach a very low level thus realizing a nearly thresholdless laser interaction [1]. In order to do that, consider that the laser action implies for each emission $\mathbf{k}_l$ mode a collective interaction of atoms with the radiation field associated with that mode. As a consequence a crucial feature of

the laser action relates to the number (or density) of StE-cooperating atoms of the medium. In this respect we believe that it is useful to postpone the main threshold-lowering argument and account first for two different cooperation processes that generally interfere with the microlaser dynamics. These processes are (a) the StE *mode competition* and (b) the *transverse quantum correlations* [1,15]. Let us consider them in detail by focusing our attention on the stimulated emission over the microcavity forward mode $\mathbf{k}_n$ with just one linear polarization.

A. Mode competition

Assume that N equal atoms are excited in the microcavity in the upper energy level and that the fluorescence time of the upper level is such that a steady-state solution of the dynamical equation represents an adequate approximation. Within the approximation of near-threshold microlaser action, viz. where all cooperative processes are weak and the gain is small, we may assume that the fraction of atoms N_n that are effective in StE over the forward mode $\mathbf{k}_n$ is given by the expression $N_n = N\eta'$, where $\eta' \equiv (\Gamma_{n,n}/\Gamma_n) < 1$. According to the definitions given in Sec. IV, $\Gamma_{n,n}$ and Γ_n are, respectively, the rates of emission over the mode $\mathbf{k}_l$ with $l = n$ and over the entire set of modes allowed by the microcavity of order n. By making use of the results of previous theory, the mode-competition coefficient η' may be calculated for various types of excitation functions $g_n(z)$

$$g_n(z) = (d)^{-1}\ , \quad \eta' = (1+2n)^{-1}$$

(uniform excitation) , (5.1)

$$g_n(z) = \delta(0)\ , \quad \eta' = [1+n+(2n)^{-1}]^{-1}$$

(laminar excitation) , (5.2)

$$g_n(z) = (2/d)\cos^2(\pi n z/d)\ , \quad \eta' = \tfrac{3}{4}[2+n+(2n)^{-1}]^{-1}$$

(periodic excitation) . (5.3)

These expressions have been calculated for a cavity order n, where n is an odd number. Similar expressions are obtained for even n. Furthermore, the above analysis only refers to the laser action in the *forward* mode $l = n$. A generalization to out-of-axis microcavity stimulated emission will presumably reproduce qualitatively the results obtained for $l = n$. We see that a decrease of the cavity length $d = n\bar{d}$ and then a reduction of mode competition implies an *increase* of the coefficient of atomic cooperation η'. This, of course, effects in a favorable manner the dynamics of the microlaser.

B. Transverse quantum correlations

The cooperation within a StE process of excited atoms belonging to a transverse section of the microcavity involves the quantum-mechanical process of the field's delocalization during emission in the proximity of a localized source. This is a subtle problem whose origin goes back to Einstein and involves the basic dynamics of the emission process as well as the very QED definition of a quantum field close to a source [15]. While postponing a detailed theoretical analysis of this process to another work, we note that the problem is generally overlooked at least in context of laser dynamics. In fact to our knowledge all laser theories developed so far appear to imply the tacit assumption that all excited atoms belonging to the transverse section of the active medium always cooperate in StE. This is to say that quantum correlations giving rise to the interatomic StE coupling extend to infinity, viz. over the full transverse (x-y) plane of Fig. 1 [14,16]. In fact we shall see that this may be approximately true for long-cavity high-Q lasers, but it is not true in general, in particular for active microcavities. Let us investigate this condition with the help of the Fig. 3, which also represents the general layout of our experiments. There it is shown that two microlasers, a distance s apart, can be excited by focusing an excitation laser beam in two different spots, of diameter $\delta \approx 10$ μm, in the transverse section of the microcavity. In the original experiment the microcavity, with finesse $f \approx 170$, was confined by plane mirrors with $|r_1|^2 = |r_2|^2 \equiv R = 99,5\%$ at λ and the excitation source was a second-harmonic generator driven by an unstable-cavity neodymium-doped yttrium-aluminum-garnet (Nd:YAG) laser delivering $\tau = 5$ nsec pulses at $\lambda_p = 0.53$ μm [15]. The StE radiation emitted at $\lambda \approx 0.63$ μm over the cavity forward $\mathbf{k}$ mode ($l = n$) was focused by a 30-cm focal-length lens, with lens aperture equal to 10 mm into a pinhole of diameter $\delta' = 10$ μm placed in front of a phototube. This provided an efficient spatial filtering against StE processes taking place on all cavity modes with $l \neq n$. The transverse-correlation problem may be reformulated by the following question: To what extend does a StE photon emitted over the common $\mathbf{k}$ mode by one microlaser determine the gain of the other microlaser, in spite of a macroscopic distance s, externally imposed on the two lasers: According to the usual theory, since a field delocalization is expected after emission over the full transversal extension of the mode, full interlaser correlation is also expected in spite of the peculiar topological configuration of the experiment [15,16]. Let us analyze the problem by considering the single longitudinal-mode case $n = 1$, for simplicity. Let m_1, m_2 denote the numbers of photons emitted by microlasers (1−2), respectively, within the coherence time $t_c = [\lambda/(v\Delta\lambda)]$ over the common k mode

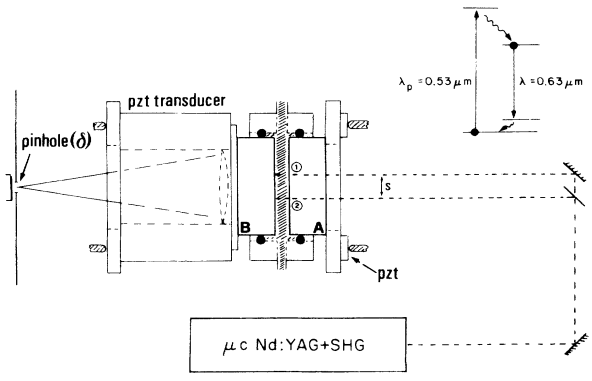

FIG. 3. Piezoelectrically (PZT) tuned Fabry-Pérot microcavity (μc) with two-beam excitation.

($\Delta\lambda \equiv$ bandwidth of the detected radiation). The time evolution equation for m_1 is given, by disregarding the cavity losses, in the simple form

$$\frac{dm_1}{dt} = G(1 + m_1 + \alpha m_2) , \tag{5.4}$$

where the degree of correlation, $\alpha = \alpha(s,d)$, $0 \le \alpha \le 1$, represents interlaser coupling. The extreme values taken by α in its existence range correspond to full laser independence and to full correlation, respectively. An identical equation holds for m_2 by interchanging indexes. At last, the overall emitted photon number $m \equiv (m_1 + m_2)$, relative to condition $\alpha = 1$, is related to $\alpha(s)$ through

$$f(s,d) \equiv [m(s,d)/m(0,d)] = 2\sinh[G(\alpha+1)]\exp[G(\alpha-1)/2]/[(\alpha+1)\sinh(2G)] , \tag{5.5}$$

where $G \equiv (gdI_p)$ is the small-signal gain proportional to the microlaser pump intensity I_p, and to d, in first approximation [16,17]. Note that the overall output gain is strongly dependent on α, as it almost *doubles* in the case of $\alpha = 1$. The measure of gain as a function of s and d is precisely the method we adopt to investigate the quantum-correlation process. By analysis of the experimental plots of the output-radiation intensity I emitted from the microcavity versus the pump intensity for various values of d and s, a progressive loss of interlaser correlation for increasing distance s was detected. The correlation loss expressed by the behavior of $\alpha(s)$ shown in Fig. 4 is found increasingly less pronounced for increasing $d > \bar{d}$, approaching asymptotically (i.e., for a macroscopic cavity $n \gg 1$) the general behavior $\alpha(s) \approx 1$ expected according to standard theory. The α curves for $d = \bar{d}$, $5\bar{d}$, $10\bar{d}$ are shown in Fig. 4 together with related best-fit Gaussian plots, which reproduce the relevant correlation, increasing behavior for increasing $d = n\bar{d}$. An approximate, simplified explanation of this behavior may be given as follows [15,18]. Consider the forward mode $l = n \ge 1$ of an active microcavity with finesse given by (2.19). This mode may be considered as a superposition of plane waves with a **k**-space distribution assigned by the Fabry-Pérot transfer function, i.e., by the Airy function $Y = |D_j|^{-2}$ given by (2.8). A simplified expression is given by $Y = [1 + (2f/\pi)^2 \sin^2\Psi]^{-1}$ and by the related expression of the Fabry-Pérot interference phase $\Psi = \pi n \cos\Theta$ as a function of the emission angle Θ (Fig. 4 inset) [8]. The full width half at maximum of the **k**-vector distribution is found to be $\Delta\Theta_n = 2(fn)^{-1/2}$. The superposition of plane waves, over each of which the forward emitted photons are delocalized, determines according to field-interference considerations, a limitation of the transversal coherence length over which StE correlations can effectively take place [18]. This process may be accounted for in simple terms by the following argument. The extent of the photon-gas Gibbs phase space corresponding to the cavity forward mode is expressed for a rectangular spatial cross section $\Delta\bar{x}\Delta\bar{y}$ by: $\Delta x \Delta y \Delta z \Delta p_x \Delta p_y \Delta p_z = h^3$, where Δz, Δp_z refer to time coordinates. This of course may be interpreted to express the minimum-uncertainty application of the Heisenberg principle to the three-dimensional dynamics of the photon particles localized with the coherence extent of the mode. By writing $\Delta p_x \Delta p_y = (\hbar k \Delta\Theta_n)^2$, we finally obtain for cylindrical symmetry the expression of the transverse quantum-correlation length $l_n = 2\lambda(fn)^{1/2}$. Then two cylindrical microlasers with diameter δ, sharing a common FP cavity mode can be coupled by StE if $l_n > \delta$. This relation leads to a further interesting insight of the dynamics of the process. In fact, if $\delta < l_n$ the cavity-allowed k-space distribution is sharper that the one requested in the nonconfinement condition by Fresnel diffraction from the circular ends of each active microlaser, or $\Delta\Theta_n < \Delta\Theta_D \approx \lambda/\delta$. Since in this case the diffraction process is made ineffective in determining the output **k** distribution, we may say that there the microcavity inhibits diffraction. The back reaction of the field to this anomalous condition consists of a kind of a coupling halo, a cylindrical region of thickness $\frac{1}{2}(l_n - \delta)$ surrounding the microlasers in which quantum correlations can take place. We refer to this condition as the cavity regime. On the other hand, if $l_n < \delta$, no StE correlation in transverse direction is possible outside the active regions. Here diffraction inhibits external correlations. This identifies the diffraction regime. Since in this regime no transversal correlation takes place over radial distances $s > l_n$, the maximum number of StE-interacting atoms is $N' = \frac{1}{4}\pi\eta' d l_n^2 = \frac{1}{2}\pi\eta' f n^2 \lambda^3$, η' being the fraction of the volume density of excited atoms corresponding to emission over the forward mode and given by (5.1), (5.2), and

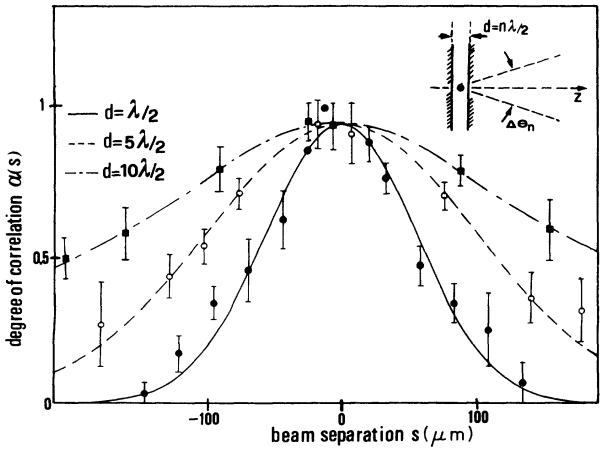

FIG. 4. Degree of Bose-Einstein quantum correlation $\alpha(s)$ as a function of the intermicrolaser distance s for microcavity spacings $d = \bar{d} \equiv \frac{1}{2}\lambda$, $d = 5\bar{d}$, $d = 10\bar{d}$.

(5.3). The above considerations lead to conclude that in open space, viz. outside a mode-selective cavity, it is impossible to detect transverse field-delocalization effects using our StE technique involving active spots apart by $l > \lambda$. There in fact the diffraction regime is always realized. In fact, by our arguments we find $l_n \approx \lambda$ for two isolated atoms cooperating in open space in the absence of external fields, in transverse photon emission, viz. emitting along a direction orthogonal to any plane to which the two atoms belong [18]. On the other hand, the use of an ideal cavity with infinite finesse leads to a single-plane-wave structure for the forward mode $\Delta\Theta_n = 0$ and to quantum correlations extending over the full transverse extent of that mode $l_n = \infty$. Furthermore, since l_n identifies a region of spatial coherence for the quantum field, including the *vacuum field*, it also identifies the transverse extent of the modes that are effectively involved in the dynamics of the single-atom SpE [3]. The cavity regime is demonstrated experimentally in Fig. 4 for increasing n. The value of f ($f \approx 170$) has been determined by direct measurement of the width of the angular distribution of the output intensity $\Delta\Theta_n$ according to classical optics [7].

VI. STEADY-STATE MICROLASER THEORY

The steady-state dynamics implied by the adoption of the mode analysis of Sec. II is justified by the relatively small value of the photon confinement time in the microcavity $\tau_{ph} = Q/\omega \approx nf/\omega$, where $Q \approx nf$ is the microcavity quality factor. The time τ_{ph}, of the order of 50 fsec for an optical microcavity, is generally far shorter than the SpE $T_0 \equiv (\Gamma_0)^{-1}$ or the other times that preside over laser dynamics [19]. We may then assume a steady-state microlaser theory which is further simplified for small n by the deterministic one-degree-of-freedom character of the coupling dynamics as remarked in Sec. I [20]. We may follow the standard theory, assuming monochromatic emission at λ over the forward mode, by adding to the rate equation (5.4) written for a single microlaser with the dominant loss term $(-m/\tau_{ph})$ according to Yariv [16,21]. Assume that the atomic excitation is provided by injecting in the cavity-active plane a pump laser beam within a focal region of diameter $\delta' < l_n$, such as full transverse correlation is established among the excited atoms. Consider that $\Gamma_{n,n}$ is the single-atom stimulated-emission rate over the forward mode $l = n$. The threshold excitation and the small-signal gain of a microlaser with spacing $d = n\bar{d}$ is immediately found to be

$$N_{th} = (2\pi c)/(n\eta'\lambda f \Gamma_{n,n}) = \pi c \Gamma_n / [\bar{d} n f (\Gamma_{n,n})^2] , \quad (6.1)$$

$$G \approx \eta' N \Gamma_{n,n} = N(\Gamma_{n,n})^2/\Gamma_n , \quad (6.2)$$

where η' is the n-dependent, mode-competition parameter given by (5.1), (5.2), or (5.3) for three different excitation density distributions. We may now insert in (6.1) and (6.2) the expressions of the emission rates evaluated in Secs. IV and V. For instance, in the case of a uniform excitation distribution $g(z) = (d^{-1})$ the above expressions lead to

$$N_{th} = [4\pi c/(\lambda f \Gamma_0)](1+2n) ,$$
$$G \approx (\tfrac{1}{2} N \Gamma_0)[n(1+2n)]^{-1} . \quad (6.3)$$

This result shows that the linear decrease of the threshold population together with the microcavity spacing $d = n\bar{d}$ comes with a dramatic increase of the microlaser gain G. the expressions (6.1), (6.2),and (6.3) represent the key results of our work. Note that this striking process does not belong to the usual laser phenomenology nor has been previously detected or anticipated theoretically in that context [1,6]. It is a quantum-mechanical phenomenon arising exclusively from the large overall *vacuum confinement* provided by the microcavity. It may therefore appear somewhat remarkable to have demonstrated by our past and present work that the Casimir-type vacuum confinement not only can affect the quantum behavior of *single* atoms, such as their spontaneous emission and Lamb's shifts, but is also able to modify, under appropriate conditions, their statistical, collective dynamical behavior. Note that the process just reported should persist as long as a virtually *complete* confinement of the field modes is determined by the cavity [2]. In Sec. VII we shall present experimental results showing that the effect is relaxed and tends to disappear for increasing cavity orders $n > 100$, i.e., when the microcavity starts becoming a trivial macrocavity.

VII. EXPERIMENTAL RESULTS

The process presented in the preceding sections has been tested by several different experiments involving different active media and different equipment. Figure 5 shows, on a semilogarithmic scale, the microcavity gain curves versus pump energy for StE at $\lambda = 0.700$ μm from oxazine-720 excited by 100-$f$sec pulses at $\lambda_p = 0.620$ μm generated by a highly stable multipass amplified

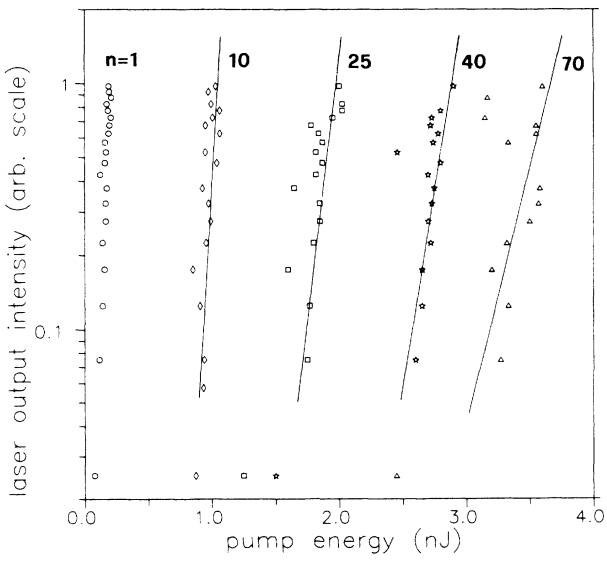

FIG. 5. Laser output intensity vs excitation energy showing, on a semilog scale, the dependence of the gain and threshold population for several cavity orders n. (Active medium: oxazine-720.)

colliding-pulse mode-locked (CPM) ring dye laser [22]. The detection system was a high-quantum-efficiency photomultiplier tube (PM) RCA C31034A-02 connected to a computer-interfaced digital-oscilloscope Tektronix 2440. The piezoelectrically (PZT) tuned microcavity was equipped with dielectric coating mirrors with diameter 25 mm and $\Theta=0$ reflectivities $R_A=R_B=0.995$ (Fig. 3). The active medium was diluted (concentration 1.2×10^{-2} mol/liter) in a drop of ethylene glycole squeezed between the mirrors. The slope of the curves drawn for different n values expresses the corresponding values of the gain G on an appropriate scale. The threshold and gain results are also reported in Fig. 6 together with a fit based on the theory given in Sec. VI. We may note the departure from the linear behavior of the threshold output energy, proportional to $N_{\rm th}$, at large values of the cavity order n, a behavior already discussed in Sec. VI showing the progressive departure from the microlaser toward the macrolaser condition due to the increasing loss of *extreme* confinement for increasing n. Equation (6.3) is adopted to evaluate the value of value of $N_{\rm th}$ for oxazine-720, $N_{\rm th}\approx5\times10^6$ for a cavity $f\approx150$ and $n=1$. This value is about one order of magnitude smaller than the result found experimentally which is $\varepsilon\approx50$ pJ, when expressed in terms of the pump short-pulse energy. As far as the gain is concerned, the discrepancy found is of the same order of magnitude as for $N_{\rm th}$. Note however in Fig. 6 the good qualitative agreement of the experimental plot presented with the theoretical results also reported there. A result similar to the one of Fig. 5, showing a still more pronounced high-gain effect, is reported in Fig. 7. This result corresponds to $f=170$ and StE at $\lambda=0.63$ μm from 4-(dicyanomethylene)-2-methyl-6-(*p*-dimethylaminostyryl)-4H-pyran (DCM) dye diluted again in ethylene-glycole pumped by a $\lambda_p=0.53$ μm, second-harmonic generation (SHG) beam under excitation by a 10-nsec pulse laser emitted by a neodymium-yttrium-aluminum-garnet laser. Note in Figs. 5 and 7 the absence of any sharp laser threshold at $n\approx1$. As discussed in Sec. I, this is related to the failure of any threshold concept (generally of any critical point for a quantum-statistical system) when the dimensionality of the mode reservoir providing damping to the system is reduced to the point that a deterministic dynamical regime becomes important [5]. Another equivalent picture of this process, already discussed in Sec. I, is provided by the failure of the very quantum-mechanical concept of spontaneous emission in the single-mode ($n=1$) microlaser. This is due to the critical realization in that dynamical condition of any vacuum state for a multiatom deexcitation [1,3]. We do not know of any other example in statistical mechanics that reproduces such a peculiar phenomenology. The above results are substantiated by our original microlaser experiment [1] and by similar, more recent experiments reported by Yokoyama *et al.* [23].

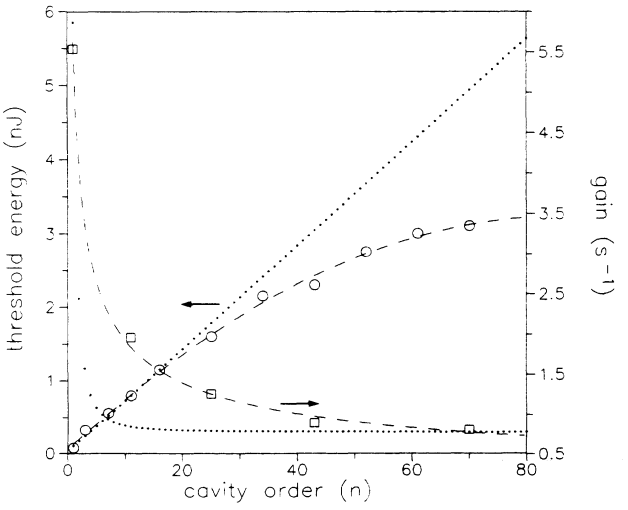

FIG. 6. Plot of gain G and threshold input energy vs the microcavity order n. The dotted curves (small dots) are calculated on the basis of the theory given in the work. They should be compared with the other two curves that merely interpolate among the experimental data.

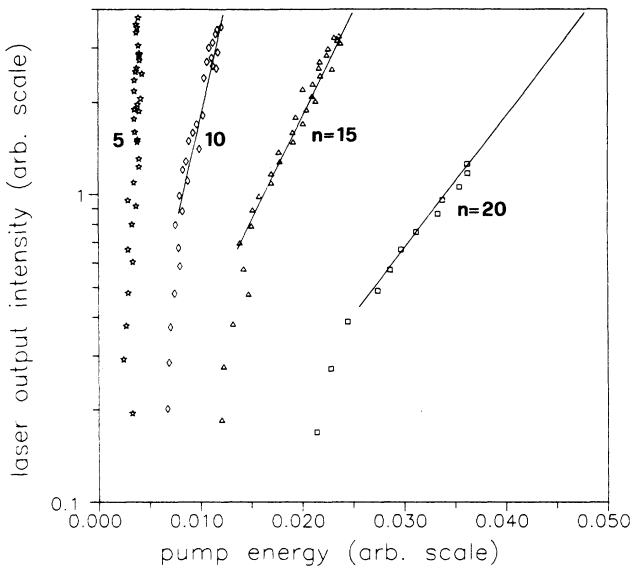

FIG. 7. Laser output intensity vs excitation energy as for Fig. 5, but corresponding to a microcavity experiment with a different active medium. (Active medium: DCM.)

A. Enhancement of spontaneous and stimulated emission by momentum-space resonant excitation: laser phase matching

The momentum-space resonant excitation and the periodic excitation method discussed at length in Sec. IV have been applied extensively to enhance the spontaneous and stimulated emission in a microcavity [11,12,13]. Let us discuss first, with some detail, the SpE process by which excited atoms placed at different positions z within the interference fringe pattern of the zero-point field at λ within the microcavity with $n=1$ decay to the ground state with a SpE time $T(z)$ that reproduces the fringe pattern. The periodic excitation technique has been adopted to control by changes of the direction of a (plane-wave) pump beam injected into the microcavity (i.e., of the injection angle Θ_p) the position of the center of mass of the distribution of atomic excitation $p(z)$

along the cavity axis. Figure 8 shows the microcavity layout. The equilateral-prism shaped FP mirror A made of quartz was multilayer coated on the plane surface belonging to the cavity to allow simultaneously for a wideband high reflectivity $R_A \approx 0.995$ (at zero incidence angle) at the SpE wavelength $\lambda \approx 6110$ Å with $\Delta\lambda/\lambda \approx 25\%$ and high transmitivity $T_{Ap} \approx 0.95$ at the excitation (pump) wavelength $\lambda_p \equiv 3547$ Å. The other cavity mirror B was coated by a silver film with thickness 530 Å to give $R_B \approx 0.95$ at both λ, λ_p. The cavity finesse was $f \approx 60$. The directional coherent pump beam, injected with field polarization parallel to the mirror plane into the interferometer through one of the oblique sides of mirror A, was provided by a third-harmonic generation of an unstable cavity, Q-switched Nd:YAG laser. The pump-pulse duration was ≈ 10 ns. At the cavity entrance the pumping beam had a Gaussian transverse profile with a width ≈ 4 mm in the SpE experiment. The cavity was tuned to $d = \bar{d}$ and aligned by PZT transducers according to previous experiments. The active medium was an europium-dibenzoylmethane complex [Eu-(DBM)$_4$] diluted in a drop of ethylene glycol squeezed among mirrors A-B. The strongest line at $\lambda = 6110$ Å (in vacuo) of the ^5D-^7F multiplet of the Eu atoms was chosen for our study [3]. The quasiexponential SpE pulses transmitted through mirror B, were detected along the cavity axis ($-z$) by a detection system similar to the one already described in this section. Each experimental data given in Fig. 9 results from a pulse-shape reconstruction obtained by the digital averaging of 2×10^3 pulse shapes detected in stationary conditions. Figure 8 displays the details of the method of periodic excitation already described in Sec. IV. For this experiment the method may be described as follows [3]. Assume that Θ is the angle between z and the pump $\mathbf{k}$ vector within the cavity $\mathbf{k}_p$. Changes of the pump-injection angle Θ_p imply changes of the wavelength $\bar{\lambda}_p(\Theta) = 2\pi/k_{pz}$, $k_{pz} \equiv |\mathbf{k}_p| \cos\Theta$ of the fringing pattern of the pump beam upon reflection on mirror B. Assuming field reflection from ideal mirrors and excitation only due to the first dominant pump fringe shown in Fig. 8, we see that the center-of-mass coordinate of the $p(z)$ distribution within the cavity can be displaced according to $z(\Theta) = \frac{1}{4}[\bar{\lambda}_p(\Theta) - \lambda]$, where $\lambda \equiv 2\pi/k$ and k are now determined within the excited medium. Then by simple changes of Θ_p the excited atoms are driven to interact with different values of the field energy density at λ, $\langle E^2(z) \rangle$, belonging to the microcavity single longitudinal mode $n = 1$. According to first-order QED perturbation theory of atom-field interactions, the probability of single-atom spontaneous emission along that mode is proportional to the zero-point energy density. For an assembly of atoms we should then expect in our case $T(z) \propto (\langle E^2(z) \rangle)^{-1}$, where the overbar means a suitable averaging over the spatial distribution of the excited atoms [9]. More precisely, the theoretical curve $\tau(z) \equiv [T(z)/T_0']$ shown in Fig. 9 representing the SpE decay time of the overall detected pulse has been determined by a rigorous computer calculation of the time superposition of the contributions due to each of the 500 spontaneously emitting plane layers orthogonal to z, by

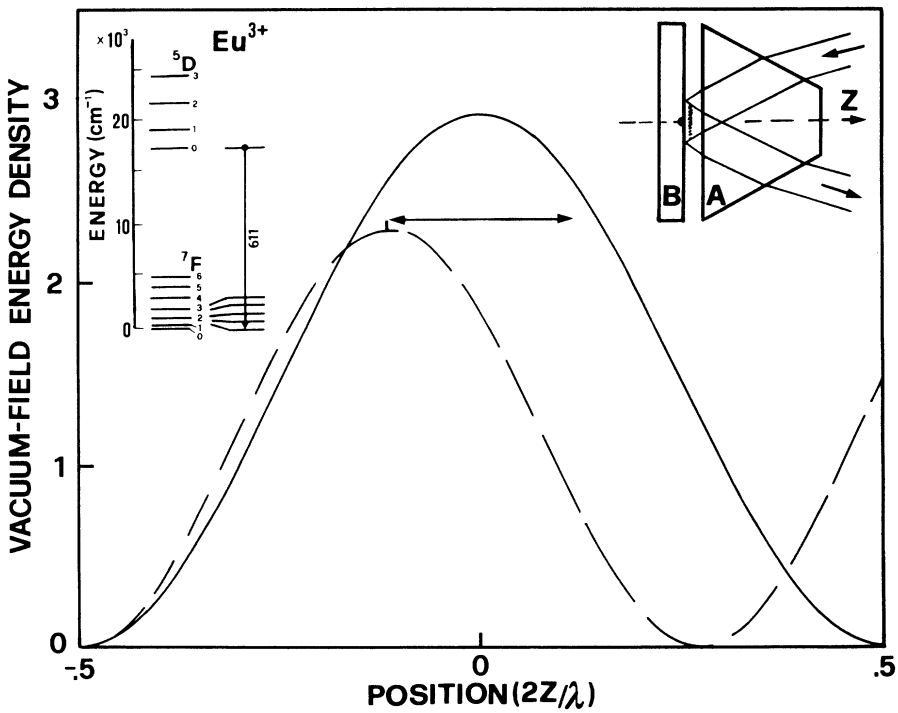

FIG. 8. Plot of the field energy density $\langle E^2(z) \rangle$ in a microcavity with spacing $d = \frac{1}{2}\lambda \equiv \bar{d}$ viz. in a spontaneous-emission-enhancement condition as for Fig. 2 (solid line). The dotted line represents the spatial distribution of excited atoms SpE or StE emitting in the microcavity and determined by periodic excitation. There the position of the center of mass of the distribution is externally controlled by acting on the injection angle of the pump beam Θ_p.

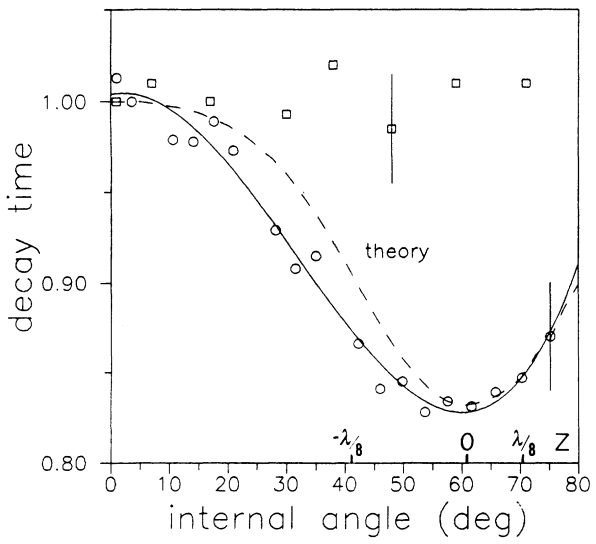

FIG. 9. Plot of the SpE time $\tau(\Theta)\equiv(T/T_0')$ relative to the value at $\Theta=0$ as a function of the angle Θ made by the pump kp vector with the z axis within a $d=\bar{d}$ microcavity [$T_0'\equiv T(\Theta=0)=530\ \mu$ s]. The square dots represent results of a falsification experiment carried out with an identical cavity but with $f\approx 0$. Several values of the z coordinate corresponding to Θ are also given.

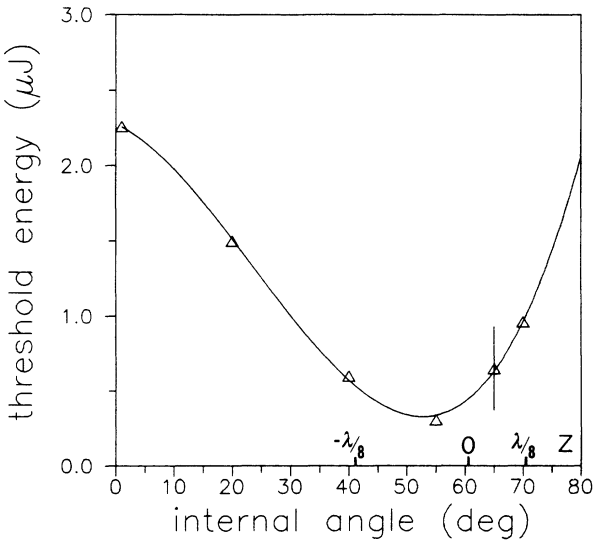

FIG. 10. Plot of the threshold pump energy as a function of Θ for the active microcavity showing evidence of the laser-phase-matching process within StE.

which to total cavity length $d\approx\bar{d}$ has been divided. The SpE-radiation pulse contributed by each layer at coordinate z decays quasiexponentially according to the value of $\langle E^2(z)\rangle$ [3]. In the calculations the effect of the *entire* pump fringe pattern established in the microcavity and the real multilayered (or metal) structure of the mirrors have been fully accounted for by use of the Lissberger-Wilcock algorithm already tested and adopted in Ref. [3]. The experimental data of Fig. 9 are found to fit well the theoretical results. The inverse bell-shaped curve with the minimum at $z\approx 0$ clearly shows the effect of the field's interference pattern. These results have been tested by a falsification procedure by three additional experiments in which the cavity field interference pattern at the SpE wavelength λ was expected to be absent while keeping the pump fringe pattern at λ_p virtually undisturbed. In the first experiment the cavity was misaligned, in a second one the cavity spacing was lengthened to the value $d\approx 15\bar{d}$, in a third one the prims mirror A was simply replaced by an equal but uncoated prism, viz. $R_A\approx 0$, $f\approx 0$. Figure 9 reports the results of the last experiment: the other ones led to similar results. There the flat $\tau(z)$ curve shows absence of any cavity-field interference at λ, as expected. An enhancement phenomenon similar to the above process has also been observed within the StE context by measuring the StE threshold $N_{\rm th}$ of our microlaser with $n=1$ in conditions similar to the ones just described but with the pump beam focused in the cavity by a 8-cm focal length lens to raise the local pump intensity at $z=0$ to $I_p\approx 500$ kW cm^{-2} (Fig. 10). The value of the threshold was determined as reported in other microlaser experiments. Figure 10 shows once again that the interplay of a phased excitation distribution with the self-interference of the field *either* in the presence or in absence of photons determines a sizable enhancement of the collective atom-field interactions. In particular we have found that the laser gain can be enhanced by our laser-phase-matching method by quite a large factor. The enhancement is found to be maximum when an exact superposition of the interference pattern at λ with the atomic excitation pattern with periodicity $\frac{1}{2}\bar{\lambda}_p(\Theta)$ is realized. This is in agreement with the theory reported at the end of Sec. IV. Of course this concept involving spatial superposition of excitation and field patterns is quite general and can be extended to more complex, three-dimensional-field modal structures in cavities of *any* size and shape. With this last work we have demonstrated that the method leads to a further improvement of the performances of the microlaser. On a more fundamental side, by this work the spatial field distribution in a cavity has been determined, either in presence or in absence of photons, i.e., in the vacuum state. From this viewpoint our SpE results provide a direct demonstration that the vacuum field exhibits the expected property of field interference [24].

VIII. CONCLUSIONS

We have reported a rather extensive investigation of the stimulated optical emission process in the microscopic Fabry-Pérot cavity. We have emphasized in the Introduction the relevance of the zero-threshold laser phase transition as a problem of statistical mechanics. Nevertheless, owing to the reduction of the dimensionality of the mode statistical ensemble, a more appropriate QED calculation of the scattering parameters giving rise to the dominant emission processes for an atomic ensemble in strong confinement condition has been undertaken. These processes are spontaneous and stimulated emissions. The expression of the rate equation for atomic emission in a microcavity has been developed, within the approximation of very high cavity Q, to determine an ex-

act dependence of the relevant parameters for the process, the gain G, and the population threshold N_{th}, on the cavity order n. The main theoretical result consists of Eqs. (6.1)–(6.3), and Fig. 6 summarizes the overall process that motivates the work. Moreover, clear evidence of the quantum-merging process of SpE into StE is provided by the $n=1$ plots in Figs. 5 and 7. We do believe that these results are determined, as said, by a peculiar synergy between several quantum-statistical processes. In our opinion they also represent a relevant achievement in modern laser physics, in particular in the field of integrated optics and related technology. The results of the theory are tested by several experiments involving different techniques inspired by the main idea of the work. The technique of laser phase matching may prove useful to externally control the coupling of atoms with the field in a microcavity. The unique dynamical behavior of the microlaser and most of its highly attractive phenomenology are expected to be reproduced by all active nonlinear optical systems whose quantum dynamics involves the concept of vacuum field in any photon creation or annihilation process. This represents quite a wide class of phenomena including the optical parametric oscillation, the free-electron laser, and generally all Compton- and Raman-type processes [25]. The extension of the concept of *extreme* vacuum confinement to Bose fields other than the electromagnetic one, e.g., to the dynamics of Cooper pairs in highly anisotropic structures in modern superconductivity, has also been proposed [26].

ACKNOWLEDGMENTS

We acknowledge the contribution of R. Tommasini and V. Cioccolanti.

[1] F. De Martini and G. R. Jacobovitz, Phys. Rev. Lett. **60**, 1711 (1988). The actual zero-threshold condition is reached asymptotically for microcavity mirror reflectivities approaching their maximum value, $R_i \to 1$. Note in this respect that a mirror reflectivity $R=0.999\,998\,4$ and a cavity finesse $f=1.9\times10^6$ at optical frequencies have been recently reported by G. Rempe, R. Thomson, J. Kimble, and R. Lalezari, Opt. Lett. **17**, 363 (1992). We intend to apply these mirrors to our microlaser. According to the theory reported in Sec. VI and to our experimental results reported in Sec. VII the use of such mirrors will lower the microlaser threshold under pulsed excitation to about 1 fJ. Owing to the value of the coherence time of the microlaser output radiation this would correspond in our case to a full realization of the peculiar quantum-statistical nearly-thresholdless phase-transition process discussed here in Sec. I.

[2] F. De Martini and G. Innocenti, in *Quantum Optics IV,* edited by J. Harvey and F. Walls (Springer, Berlin, 1986); Quantum Electron. Conf. (IQEC) Tech. Digest **XIV**, 147 (1986); F. De Martini, G. Innocenti, and P. Mataloni, IQED Tech. Digest **XV**, 128 (1987); F. De Martini, G. Innocenti, G. Jacobovitz, and P. Mataloni, Phys. Rev. Lett. **59**, 2955 (1987); W. Jhe, A. Anderson, E. A. Hinds, D. Meschede, L. Moi, and S. Haroche, *ibid.* **48**, 666 (1987); E. Yablonovitch, *ibid.* **58**, 2059 (1987); M. R. Philpott, Chem. Phys. Lett. **19**, 435 (1973); G. Barton, Proc. R. Soc. London, Ser. A **320**, 251 (1970); Phys. Scr. **T21**, 11, (1988); P. W. Milonni and P. L. Knight, Opt. Commun. **9**, 119 (1973).

[3] F. De Martini, M. Marrocco, P. Mataloni, L. Crescentini, and R. Loudon, Phys. Rev. A **43**, 2480 (1991). The work of X. P. Feng and K. Ujihara, IEEE J. Quantum Electron. 25, 2332 (1989) is restricted to one-dimensional calculations that cannot adequately represent the spatial distribution of SpE and StE in a microcavity.

[4] Casimir-type *extreme* confinement is realized for any field confinement over a space-time length λ_D the de Broglie wavelength of the corresponding particle. Examples are the microcavity, all kinds of particle diffraction, electrons in multiple-quantum-well structures, phonon trapping in highly anysotropic crystals, cf. F. De Martini, Phys. Scr. **T21**, 58 (1988). The microcavity single-mode concept is an approximate one because waveguide-type "radial" modes propagating in directions parallel to mirrors with polarization orthogonal to them are also allowed. However they are unaffected by cavity resonance and have been found experimentally to be weakly excited for $d=\bar{d}$. In our SpE experiments the radiation loss determined by the "radial" modes for $n \leq 10$ has been found to be of the order of 3%.

[5] W. H. Louisell, *Quantum Statistical Properties of Radiation* (Wiley, New York, 1973), Chaps. 6 and 8.

[6] M. Sargent, III. M. O. Scully, and W. E. Lamb, *Laser Physics* (Addison-Wesley, Reading, MA, 1974), Chap. 16; V. De Giorgio and M. O. Scully, Phys. Rev. A **2**, 1170 (1970); J. F. Scott, M. Sargent III, and C. Cantrell, Opt. Commun. **15**, 13 (1975). Note that in the passage from nonequilibrium to equilibrium problems there is a sign reversal in the inequalities involving reservoir variables and corresponding to the same phase. Then the zero-threshold condition $N_t=0$, implying nonexistence of the "incoherent-field phase," corresponds analogously to an infinite value of the equilibrium "order parameter" T_c. The concept of "negative temperature" in early maser theory is related to this analogy.

[7] M. Born and E. Wolf, *Principles of Optics* (Macmillan, New York, 1964), Chap. 7. The "finesse" should be taken as a useful but approximate concept within the context of our present cavity theory which considers large angles Θ and different $|r_j|$ for different field polarizations.

[8] In the "enhancement" condition, i.e., for n a whole number, d is the actual physical spacing of the FP cavity only when this one is bounded by lossless, infinitely thin mirrors, as in the case of metal coatings. In the case of thick, multilayer coatings, d may be taken as the distance between two parallel ideal reference planes close to the plane surfaces of the actual mirrors that reproduce the field-phase condition of equivalent thin, lossless mirrors. This equivalence condition is discussed at Ref. [3] for spontaneous emission. The wavelength λ appearing in all expressions in Sec. III and following is defined within the lasing material with refractive index $\bar{n}$, viz., is related to the vacuum wavelength λ_0 by $\lambda=\lambda_0/\bar{n}$.

[9] R. Loudon, *The Quantum Theory of Light,* 2nd ed. (Oxford University Press, New York, 1983).

[10] Y. Yamamoto, in Proceedings of the International Quantum Electronics Conferences, Anaheim, California, 1990 (unpublished); Y. Yamamoto, S. Machida, K. Igeta, and G. Bjork, in *Coherence, Amplification, and Quantum*

Effects in Semiconductor Lasers, edited by Y. Yamamoto (Wiley, New York, 1991). The "spontaneous-emission parameter" β reported in these works coincides with the "mode-competition" coefficient η' adopted in our work.

[11] The spectroscopy in the momentum space was first introduced in context of nonlinear spectroscopy of the polaritons in solids by J. P. Coffinet and F. De Martini, Phys. Rev. Lett. **22**, 60 (1969).

[12] A. Kastler, Appl. Opt. **1**, 17 (1962); F. De Martini, Phys. Lett. A **115**, 421 (1986).

[13] For cavity orders expressed by even numbers the "periodic excitation" technique give favorable results for atomic excitation distributions symmetric with respect to $z=0$ and peaked at $z=l''d/(2n)$ where $l''<n$ is an odd number.

[14] The somewhat large Γ_n value reported in Ref. [2] is likely due to an incipient thresholdless merging of SpE into StE.

[15] F. De Martini, M. Marrocco, and D. Murra, Phys. Rev. Lett. **65**, 1853 (1990). The QED photon-delocalization model was first introduced by A. Einstein, Phys. Z. **18**, 121 (1917). An analysis of the transverse interatom correlation based on the coupled Heisenbergs problem in a microcavity will be reported elsewhere.

[16] A. Yariv, *Quantum Electronics* (Wiley, New York, 1967), Chap. 15; F. Shafer and W. Smith, Phys. Lett. **9**, 306 (1966). In our experiment $t_c \approx 1.5$ psec, the retardation time between microlasers 100 μm apart is $t_r \approx 0.5$ psec; then $t_r \ll \tau$, the pump pulse duration. This implies that the reduction of StE correlation for $s>0$ cannot be attributed to trivial retardation in the radial direction. Note the peculiar field-retardation process taking place in the experiment (Ref. [14]). In an idealized situation, a photon emitted by microlaser 1 cannot interact with 2 in a time shorter than t_r, as a StE correlation corresponds to information exchange between lasers. Information transfer is certainly provided by photons belonging to the cavity radial modes. However, StE effects taking place on radial modes cannot be detected by our highly efficient lens-pinhole spatial filter. For retardation in atom-radiation processes, cf. E. Fermi, Rev. Mod. Phys. **4**, 7 (1932); S. Kikuchi, Z. Phys. **66**, 8 (1930); M. Fierz, Helv. Phys. Acta **23**, 731 (1950); P. Milonni and P. Knight, Phys. Rev. A **10**, 4 (1974); V. P. Bykov, Usp. Fiz. Nauk. **143**, 657 (1984) [Sov. Phys. Usp. **27**, 631 (1984)].

[17] A detailed space-time study on the Bose-Einstein interlaser correlation process in the femtosecond time scale is presently in progress in our quantum-optics laboratory in Rome. The nonlocality of the field investigated by our new transverse-correlation technique may be related to a quantum nonseparability process, cf. A. Einstein, B. Podolsky, and N. Rosen, Phys. Rev. **47**, 777 (1935); M. Jammer, *The Philosophy of Quantum Mechanics* (Wiley, New York, 1974); F. De Martini, in Proceedings of the Niels Bohr Symposium [Riv. Storia Sci. **2**, 557 (1985)].

[18] An equivalent, rigorous approach for the determination of the l_n is provided by Feynman path-interference considerations related to the coupling problem. There *each* path corresponds to a single deexcitation channel, viz., to a single **k** vector available for atom deexcitation. Exactly for this reason the localization effect (or, $l_n < \infty$) found in Ref. [14] depends on the spatial mode structure of the field coupled to the excited atom. This structure is determined by the external boundary conditions, e.g., by the presence of a mode-selective cavity. R. P. Feynman and A. Hibbs, *Quantum Mechanics and Path Integrals* (McGraw Hill, New York, 1965), Chap. 1; K. Huang, *Statistical Mechanics* (Wiley, New York, 1963), Chap. 9. With usual macroscopic cavities, $n \gg 1$ and $l_n \gg \lambda$; e.g., with $f=100$, $d=10$ cm, $\lambda=0.7$ μm we have $l_n \approx 1$ cm.

[19] The value of the SpE times of the media adopted in our microlasers span a range from several nanoseconds (rhodamine-type dyes) to hundreds of microseconds [$T_0=560$ μsec for Eu-$(DBM)_4$ complex]. Of course, the dynamics of the atomic-coherence processes, such as superfluorescence and superradiance, may involve the much shorter "transverse" relaxation times which range from about $T_2^* \approx 50$ fsec (rhodamine) to $T_2^* \approx 400$ fsec [Eu-$(DBM)_4$ complex] at 300 K, cf. C. H. Brito Cruz, R. L. Fork, W. H. Knox, and C. V. Shank, Chem. Phys. Lett. **132**, 341 (1986); L. Allen and J. H. Eberly, Optical Resonance and Two-Level Atoms (Dover, New York, 1975), Chap. 7.

[20] For $n=1$ the coupled Heisenberg equations expressing the microlaser dynamics can be solved in closed form, as remarked in Ref. [1].

[21] Owing to the bound-system character of active media adopted in our microlaser, fluorescence damping processes due to atomic or molecular confinement (surface effects) are negligible. However, in solid-state microlasers, geometry-dependent exciton-recombination effects can be a severe source of loss that may partially undermine the intrinsic thresholdless character of the device. R. E. Slusher, private communication and Proceedings of the Optical Society of America Annual Meeting, Boston, MA 1990 (unpublished).

[22] P. Mataloni, M. Santosuosso, and F. De Martini, Appl. Phys. B **52**, 273 (1991).

[23] H. Yokoyama, S. D. Brorson, E. Ippen, Y. Nambu, and M. Suzuki, in *Nonlinear Optical Materials: Physics, Materials, and Applications,* edited by S. Miyata (Elsevier, New York, 1992). We should give reference to two short and unpublished conference abstracts by T. Kobayashi, edited in mimeographed form and in Japanese, in Technical Digest of the 43th Fall Meeting of the Japanese Applied Physics Society (1982) and in Technical Digest of 46th Fall Meeting of Japanese Applied Physics Society (1985). These short abstracts report a very qualitative but correct proposal for laser application of the field-confinement process arising in several microcavity configurations. No detailed calculations or experimental realization of the microlaser or of similar devices are reported there.

[24] A comprehensive account of the role of the *vacuum field* in atomic phenomena is found in *Foundations of Radiation Theory in Quantum Electrodynamics,* edited by A. Barut (Plenum, New York, 1980).

[25] F. De Martini, in *Free Electron Lasers,* edited by W. B. Colson, C. Pellegrini, and A. Renieri (North-Holland, Amsterdam, 1990). A micro-optical parametric oscillator and the Raman effect in complete vacuum-confinement condition are presently being investigated in a joint collaboration between C.N.E.T. Laboratories in Paris and our laboratory in Rome.

[26] F. De Martini, Phys. Scr. **T21**, 58 (1988); Phys. Rev. Lett. **60**, 1711 (1988); A. Bianconi, M. De Santis, A. Di Cicco, A. Flank, A. Fontaine, B. P. Lagarde, and H. Katayama-Yoshida, Phys. Rev. B **38**, 7196 (1988).